NREL/CP-510-22943 • UC Category: 1250

Effect of Front-Surface Doping on Back-Surface Passivation in $Ga_{0.5}In_{0.5}P$ Cells

S.R. Kurtz, J.M. Olson, D.J. Friedman,
and R. Reedy
Presented at the 26th IEEE Photovoltaic
Specialists Conference, September 29–
October 3, 1997, Anaheim, California

National Renewable Energy Laboratory
1617 Cole Boulevard
Golden, Colorado 80401-3393
A national laboratory of
the U.S. Department of Energy
Managed by Midwest Research Institute
for the U.S. Department of Energy
under contract No. DE-AC36-83CH10093

Prepared under Task No. PV702601

September 1997

EFFECT OF FRONT-SURFACE DOPING ON BACK-SURFACE PASSIVATION IN $Ga_{0.5}In_{0.5}P$ CELLS

Sarah R. Kurtz, J. M. Olson, D. J. Friedman, and R. Reedy
National Renewable Energy Laboratory, Golden, Colorado

ABSTRACT

The emitter doping of a solar cell usually affects the blue response of the cell because the blue light is strongly absorbed at the front of the cell in the emitter layer. However, we show here that changing the identity of the dopant at the front of the cell affects the performance of the back of the cell, sometimes more than the performance of the front of the cell. Specifically, a highly Zn-doped $Ga_{0.5}In_{0.5}P$ layer makes a good back-surface field in an n-on-p $Ga_{0.5}In_{0.5}P$ cell with Se doping, but not when Si doping is used, consistent with the results of Takamoto, et al. During growth of the n-type layers, Zn diffuses up through the cell, piling up at the junction. When Si doping is used, the diffusion is enhanced.

INTRODUCTION

$Ga_{0.5}In_{0.5}P$/GaAs cells, invented and developed at the National Renewable Energy Laboratory, have achieved efficiencies of 30.3% [1], 25.7% [2], and 30.2% [3] for AM1.5 Global, AM0, and concentrator conditions, respectively. Most of these cells used a highly Zn-doped $Ga_{0.5}In_{0.5}P$ (hereafter, GaInP) layer as a back-surface field (BSF) for the GaInP cell [4]. The passivation of the back of this cell is especially important because it is usually grown thin to match the photocurrents of the GaInP and GaAs cells. The highly Zn-doped layer passivates because (1) higher doping moves the Fermi level closer to the valence band, and (2) the higher Zn doping causes the band gap of the GaInP layer to increase [5]. Takamoto, et al. were unable to passivate the back of the GaInP cell with the highly doped GaInP layer, unless a thick (0.3 μm) layer was used in the GaInP/GaAs cell structure (they did not have difficulty with the GaInP single-junction cell) [6]. They identified the problem as diffusion of the Zn out of the BSF, into the base. After diffusion, the BSF layer was reduced in doping, and lower photocurrent and voltage were obtained. The success of the earlier work [2] at using the Zn-doped GaInP for a BSF, and the failure of Takamoto's attempt with a similar structure was a puzzle until we substituted Si for Se as the n-type dopant in the GaInP cell. When we use Si and our standard recipe, like Takamoto, et al., we find that the Zn-doped GaInP layer no longer passivates the back of the cell.

Growth of an n-type layer was shown to cause anomalous diffusion in underlying Zn-doped layers as early as 1988 [7]. Deppe put forth an explanation for this effect in 1990 [8]: Fermi-level pinning at the growth surface causes the grown-in point-defect concentration to be different from the bulk equilibrium point-defect concentration. Specifically, during growth of the n-type layers, the Fermi level is pinned near the middle of the gap at the surface, but moves toward the conduction band as growth proceeds and the layer becomes part of the bulk. This creates an excess of Ga interstitials, which then move into the lower p-type layers. The Ga interstitials "kick-out" the Zn atoms, freeing them to move quickly through the p-type layer. Although this explanation is widely accepted, there is little agreement about the details, including the charge states of the interstitials [9, 10], the role of vacancies [11], and the reasons for different behavior at different growth temperatures [12-14].

One of the unanswered questions is why the identity of the n-type dopant (Si or Se) would change the Zn diffusion. Fujii, et al., showed that less diffusion occurs when Si rather than Se is used [14], the opposite of the result we describe here. Fujii's result was obtained with a higher temperature, 750°C, and a different material system, GaAs/AlGaAs, and differs in other ways as well. They observe no diffusion of the Se, whereas we observe Se diffusion; they show the Zn diffusing into the n-type layer, whereas we observe the Zn piling up on the p-type side of the junction.

In this paper, we describe the changes in the cell performance that are correlated with the use of Si and with growth conditions that increase the diffusion. The diffusion is shown graphically by secondary ion mass spectroscopy (SIMS) measurements. We also show how similar effects are observed for GaAs cells and discuss the diffusion, how it can be controlled, and a possible explanation for the difference between Si and Se doping.

EXPERIMENTAL DETAILS

Single-junction n-on-p GaInP and GaAs cells were grown by atmospheric-pressure, metalorganic chemical vapor deposition using trimethylgallium, trimethylindium, trimethylaluminum, arsine, and phosphine. Palladium-purified hydrogen was used as a carrier gas and diethylzinc, hydrogen selenide, and disilane were used as the dopant sources. Table 1 describes the growth sequence for the GaInP cells.

Table 1. Growth sequence for GaInP cells a, b, c, and d. The growth was at 600°C for the first two layers and 700°C for the rest.

Layer	Mat.	Thick (μm)	Dopant	Growth rate (μm/hr)	Group V Press. (torr)
Buffer	GaAs	0.2	Zn^+	2.2	2
BSF	GaInP	0.05	Zn^+	4.4	1.5
Base	GaInP	0.84	Zn	4.4	4.4
	GaInP	0.007		4.4	4.4
Emitter	GaInP	0.09	Si (b,d) Se (a,c)	4.4	2.8
Window	AlInP	0.025	Si^+	4.4	9
Cap	GaAs	0.5	Si^+ (b,d) Se^+ (a,c)	3.3 (a,b) 6.6 (c,d)	0.1 (a,b) 0.5 (c,d)
Cooling	As				0.1, 0.5

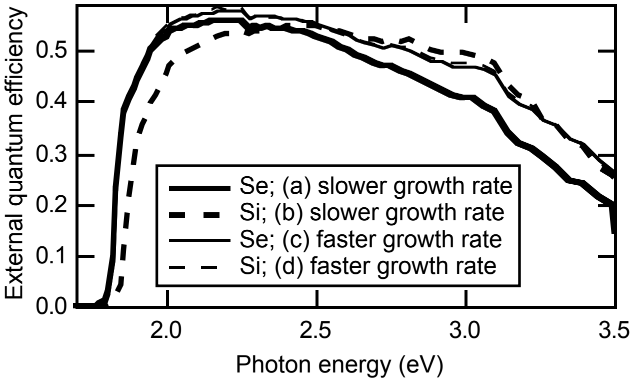

Fig. 1. The effect of Si or Se dopant in the cap and emitter layers on the external quantum efficiency of four uncoated GaInP cells. The caps for the samples labeled "slower growth rate" were grown at 3.3 µm/hr and lower arsine pressure and are expected to show more diffusion than those grown at 6.6 µm/hr.

The quantum efficiency was measured in the dark with zero voltage bias using a monochromator and lock-in detection on cells without antireflection coatings. The current-voltage (I-V) measurements were made under a solar simulator using a GaInP reference cell. The sheet resistance measurements used transmission lines adjacent to the devices. The base doping levels were measured from the capacitance as a function of voltage for the finished devices. The SIMS measurements used a Cs^+ beam and the masses 28 for Si, 31 for P, 64 for Zn, 75 for As, and 80 for Se. The SIMS concentration calibrations were estimated due to the lack of Se, Si, and Zn:GaInP SIMS standards. Relative sensitivity factors were calculated for the dopants in GaInP based on published doped GaP and InP sensitivity factors [15]. The absolute dopant concentrations should be accurate to within 15%-20%.

RESULTS

Figs. 1-3 compare the performance of four GaInP cells using Se or Si in the emitter and cap layers for two different cap designs. Although changing the emitter dopant would be expected to change the (blue) response of the emitter, Fig. 1 shows significant changes in the base (red) as well. The reduction in red response, when Si ((b) in Fig. 1) is substituted for Se ((a) in Fig. 1) is very reproducible for this cell recipe. The conditions used for growth of the cap are most important; the conditions used for the emitter growth are less important in determining the red response. When low-diffusion conditions are used no change is observed in the quantum efficiency ((c) and (d) in Fig. 1).

The poor red response observed in Fig. 1 for sample (b) is correlated with the "light-induced" shunt shown in Fig. 2. The curves in Fig. 2 were adjusted by adding the short-circuit current to the I-V curve measured under 1-sun illumination. For an ideal diode, the voltage-dependent current, I(V), can usually be modeled from the dark current, Idark(V), according to

$$I(V) = Idark(V) - Iphoto,$$

where Iphoto is the short-circuit current. However, if this were the case, the two curves for sample (b) in Fig. 2 would lie on top of each other. This "light-induced" shunt is evidence of field-aided collection; we observe an increase of the quantum efficiency with reverse bias. A similar, although less pronounced, "light-induced" shunt is observed for GaAs cells using a Si-doped GaAs emitter and GaInP for passivating the front and back.

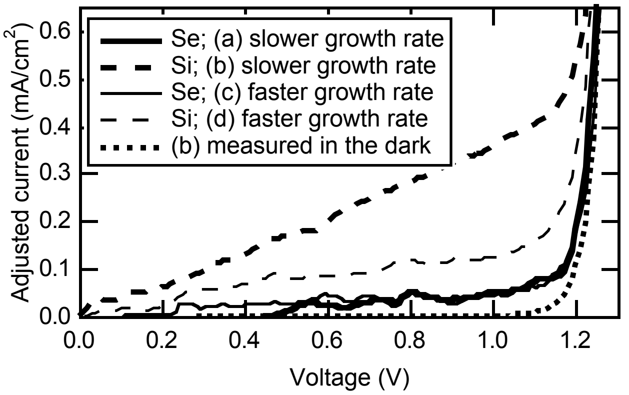

Fig. 2. One-sun, current-voltage curves for the same devices described in Fig. 1. Each curve was adjusted by adding the short-circuit current. The bottom curve was measured in the dark.

Sample (b) also has an increased base doping relative to the other three cells, as shown in Fig. 3. The origin of this increased hole concentration is shown by SIMS measurements to be Zn diffusion (Fig. 4). Samples (a) and (c) (Se doping) have Zn profiles that are very close to the intended ones (Table 1). However, the Zn in samples (b) and (d) (Si doping) has moved out of the underlying p-type layers into the base. Compared with sample (d), the slower growth and lower arsine pressure used for the cap layer of sample (b) causes more Zn diffusion with the Zn piling up in the depletion region associated with the n-p junction.

Additional GaInP-cell data are summarized in Table 2 and plotted in Fig. 5. The expected increase of V_{oc} with band gap is observed for GaInP cells grown with similar caps. However, samples with cap (b), using slower growth rate and lower arsine pressure, show higher band gaps, decreased red response, and, on average, 40 mV less V_{oc} for a given band gap, compared with cap (a). The run-to-run variation of the band gap-adjusted V_{oc} is about 10 mV.

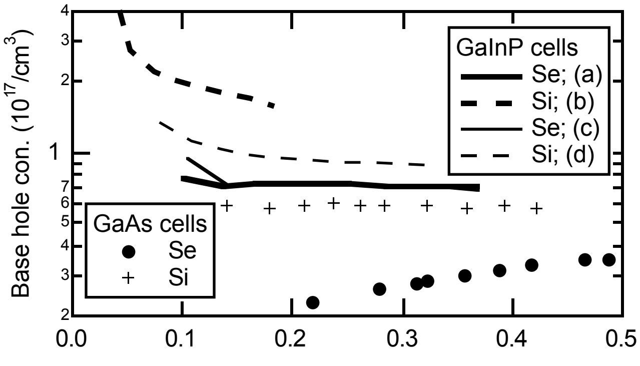

Fig. 3. Hole concentration as measured by capacitance-voltage profiling for samples a-d and for two GaAs cells. The legends identify the dopant used in the cap and emitter. The depth is the depletion width calculated from the capacitance.

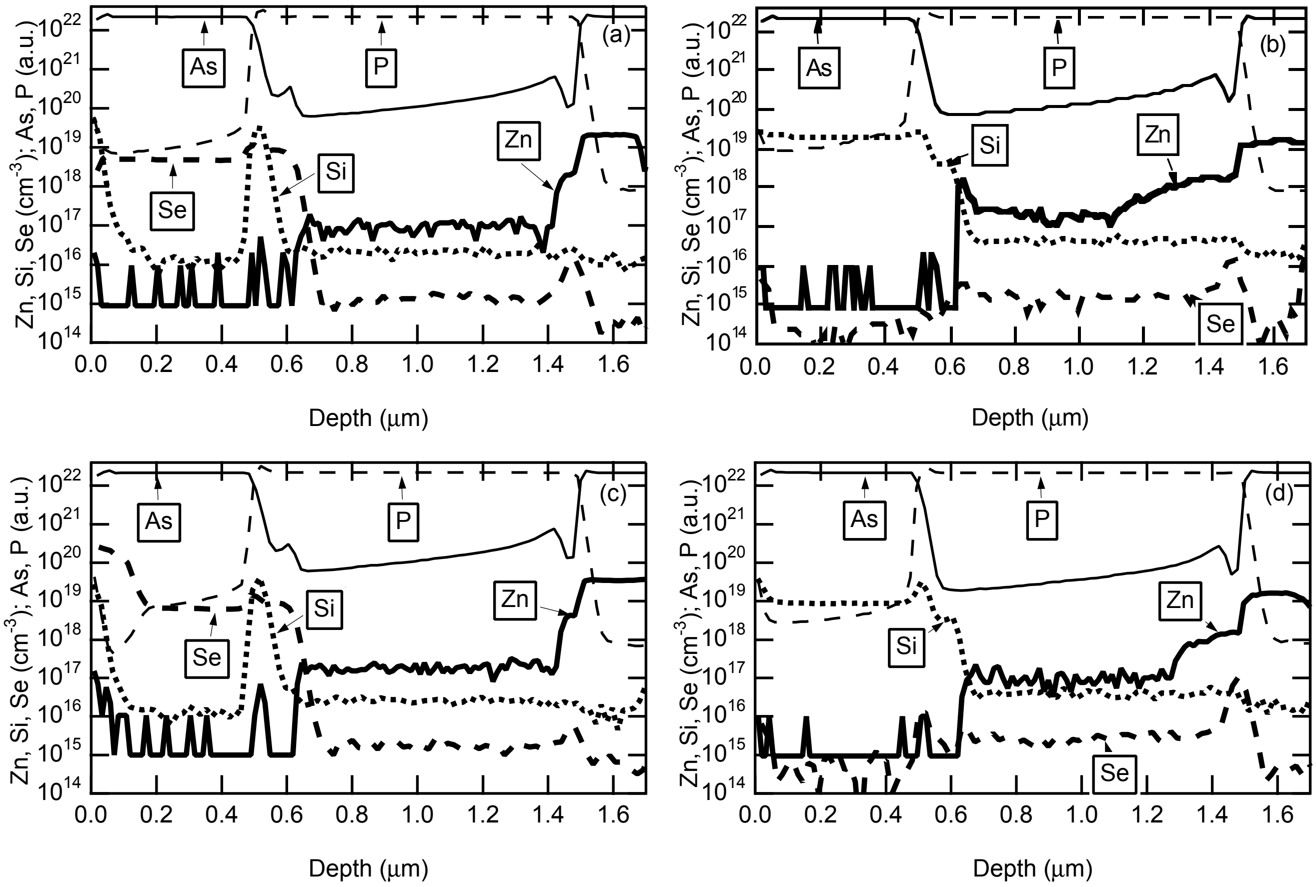

Fig. 4. SIMS profiles for same samples as Figs. 1-3. The device structures are described in Table 1.

Table 2. The band gap, red response, V_{OC}, and emitter sheet resistance for a number of GaInP cells. The first four samples are the same as those described above. The rest of the samples were grown the same as (b) with minor modifications: (e) used a lower phosphine flow during growth of the base, (f) included an anneal between growth of the base and the emitter, (g) used lower disilane flows in the emitter and cap, and (h) used higher disilane flow in the emitter.

Sample	Dopant	Eg (eV)	Red	V_{OC} (V)	Emitter (Ω/sq)
(a)	Se	1.824	+	1.325	204
(b)	Si	1.856	-	1.320	456
(c)	Se	1.825	+	1.335	186
(d)	Si	1.826	+	1.320	387
repeat(b)	Si	1.859	-	1.330	401
(e)	Si	1.863	-	1.330	451
(f)	Si	1.864	-	1.325	450
(g)	Si-	1.832	+	1.340	531
(h)	Si+	1.874	-	1.339	438

Somewhat similar effects are also observed for GaAs cells. Table 3 shows data for four GaAs cells with GaInP emitter and 1-μm-thick GaAs base (making these heterojunction devices). The variation in photocurrent for these GaAs cells is not detectable. However, the V_{OC}s vary and are higher when more Se is used, consistent with the GaInP results. The dark currents associated with the V_{OC}s reported in Tables 2 and 3 show a diode factor of unity. Table 3 also includes data for two GaAs homojunctions with GaInP front and back passivation. The hole concentrations measured for these two samples are shown in Fig. 3.

Tandem GaInP/GaAs cells show similar changes when Si is substituted for Se. The top-cell red response is good for a Si-doped tandem if low diffusion conditions are used. However, we have not identified a set of conditions (with GaInP BSF) that gives a high V_{OC} when Si is used.

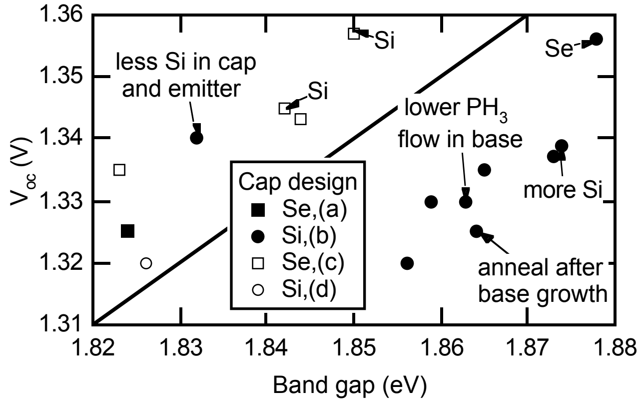

Fig. 5. V_{OC} as a function of measured band gap. The conditions for the cap growth are specified in the legend. The tags specify the doping in the emitter or another change. Samples below the line have poor red response.

Table 3. Properties of GaAs cells with GaAs or GaInP emitters and Si or Se doping. The red responses did not vary for the heterojunction cells. The Si-doped homojunction showed poor blue response, consistent with the high emitter doping.

Cap	Emitter	V_{OC}	Emitter sheet res. (Ω/sq)	Cap sheet res. (Ω/sq)
Se,(c)	Si:GaInP	1.028	403	20
Si,(b)	Si:GaInP	0.999	325	9.5
Se,(c)	Se:GaInP	1.033	292	18
Si,(b)	Se:GaInP	1.012	478	9.6
Si,(c)	Si:GaAs	0.96	45	6.9
Se,(c)	Se:GaAs	1.04	59,87	9.5,7.6

DISCUSSION

When Zn diffuses all the way through the base of a GaInP cell (as observed for sample (b), Fig. 4), the band gap of the GaInP base increases because of group III disordering [16], and the heavily Zn-doped GaInP BSF ceases to be distinguishable from the adjacent base. The symptoms of Zn diffusion all the way through the base include an increase in band gap and poor red response (Fig. 1), shunted light I-V curves (Fig. 2), increased hole concentration (Fig. 3), and lower V_{OC} (Fig. 5). Diffusion in a GaAs cell causes no change in red response (the band gap of GaAs is insensitive to group III diffusion), but slight shunting of the light I-V curves and changes in the V_{OC} can be observed. The pile up of Zn in the field region at the n-p junction may be caused by a higher group III vacancy concentration for the higher Fermi level in the junction region [11]. Interstitial Zn atoms move through the p-type layer until they either find a group III vacancy or until they "kick out" a group III atom.

The smaller amount of Zn diffusion seen for sample (d) in Fig. 4 causes no measurable change in the band gap or quantum efficiency (Fig. 1). However, a slight shunt is still observed in the light I-V curve (Fig. 2), and the increase in hole concentration (Fig. 3) and loss in V_{oc} (Fig. 5) are still measurable, but small. When the Zn diffusion is small, the Ga and In remain somewhat ordered on their sublattice, preventing the striking change in band gap. Although Fig. 1 shows no measurable change in quantum efficiency for sample (d) compared with sample (c), the red response at the maximum-power point has changed (Fig. 2 shows a slightly shunted I-V curve for (d), implying that the quantum efficiency measured in forward bias will be less than that measured at zero bias.)

Takamoto, et al., [1] have shown that the diffusion can be reduced and record-efficiency devices obtained by using a Zn-doped AlInP BSF. Nevertheless, it would be useful to understand how to control the diffusion in other ways and to understand why Si causes more diffusion than Se. We observe that the diffusion can be reduced by (1) decreasing the growth time of the n-type layers, (2) increasing the group V pressure during growth of the n-type layers, (3) reducing the doping of any layer, or (4) inserting a diffusion barrier (e.g., the window or BSF). The diffusion is relatively unaffected by the group V pressure during growth of the base layer or by a growth interrupt between the p- and n-type layers, as shown in Table 2 and Fig. 5. Tandem cells contain two sets of n-type layers, both of which will contribute to the diffusion.

Diffusion in III-V devices during growth is very complicated and has been extensively reported in the literature. However, the role of Se diffusion in causing Zn diffusion has not been discussed much. Se is reported to diffuse less than Si. Although there is always some memory effect associated with Se, the data show clearly that Se diffuses under common growth conditions. A possible explanation for both the reason why Se diffuses and why less Zn diffuses when Se is present is that some of the excess Ga interstitials from the n-type layers may undergo the following reaction

$$\mathrm{Ga_I + Se_{As} \text{-->} Ga_{As} + Se_I} \qquad (1),$$

where the subscripts I and As denote an interstitial or an atom sitting on an arsenic site, respectively.

Northrup, et al. calculate that Ga on an As site is relatively stable in n-type GaAs [10]. Se_I is likely to be the diffusing species for the Se diffusion (group V vacancies could also allow Se to diffuse). If the Se_I does not generate another Ga_I, reaction (1) represents a decrease in the available Ga_Is, possibly explaining the decrease in Zn diffusion when Se, rather than Si doping is used.

SUMMARY

Replacing Se doping with Si doping in the cap and emitter layers enhances diffusion of Zn from the back of the cell into the base. The symptoms of Zn diffusion from the back to the front of the GaInP base include an increase in the GaInP band gap, a decrease in the red response, shunting of the light I-V curve, increased base doping near the junction, and decreased V_{OC}. Smaller amounts of diffusion increase the base hole concentration slightly, decrease the fill factor slightly, and degrade the V_{OC} by 10-20 mV. The Zn diffusion can be reduced by using Se instead of Si, decreasing the growth time or increasing the group V pressure during growth of the n-type layers, decreasing the doping of any layer, or adding a diffusion barrier either at the front or the back of the cell. The conditions for the cap growth are more important than those of the emitter. Tandem cells using Si doping and a highly Zn-doped GaInP layer for the back-surface field were fabricated with good photocurrents and fill factors, but the open-circuit voltages were still inferior compared with when Se doping is used. A complete understanding of the Zn diffusion is still lacking.

ACKNOWLEDGEMENTS

We thank C. Kramer for growth and processing of the devices and S. Batra for help with data collection. This work was performed under DOE contract number DE-AC36-83CH10093.

REFERENCES

[1] T. Takamoto, et al., *Appl. Phys. Lett.*, **70**, 1997, p. 381.
[2] K. Bertness, et al., *Appl. Phys. Lett.*, **65**, 1994, p. 989.
[3] D.J. Friedman, et al., *Progress in Photovoltaics: Research and Applications*, **3**, 1995, p. 47-50.
[4] D.J. Friedman, et al., *22nd IEEE PVSC*, 1991, p. 358.
[5] S.R. Kurtz, et al., *J. Electron. Mater.*, **23**, 1994, p. 431.
[6] T. Takamoto, et al., *First World Conference on Photovoltaic Energy Conversion*, 1994, p. 1729-1732.
[7] P. Enquist, et al., *J. Appl. Phys.*, **63**, 1988, p. 4485.
[8] D.G. Deppe, *Appl. Phys. Lett.*, **56**, 1990, pp. 370-372.
[9] R.M. Cohen, *J. Appl. Phys.*, **67**, 1990, p. 7268.
[10] S.B. Zhang, et al., *Phys. Rev. Lett.*, **67**, 1991, p. 2339.
[11] N.N. Grigorev, et al., *Semiconductors Engl. Tr.*, **31**, 1997, pp. 595-599.
[12] R. Bhat, et al., *Appl. Phys. Lett.*, **65**, 1994, p. 338.
[13] K. Kurishima, et al., *J. Appl. Phys.*, **79**, 1996, p. 4017.
[14] N. Fujii, et al., *J. Cryst. Growth*, **145**, 1994, p. 808.
[15] R.G. Wilson, et al., "*Secondary Ion Mass Spectrometry: a practical handbook for depth profiling and bulk impurity analysis*," (Wiley, New York, 1987).
[16] A. Gomyo, et al., *Appl. Phys. Lett.*, **50**, 1987, p. 673.